Structural Analysis of Historic Construction – D'Ayala & Fodde (eds)
© 2008 Taylor & Francis Group, London, ISBN 978-0-415-46872-5

The structural behaviour of masonry vaults: Limit state analysis with finite friction

D.F. D'Ayala
Department of Architecture and Civil Engineering, University of Bath, UK

E. Tomasoni
University of Brescia, Italy

ABSTRACT: The increasing interest in historic architectural heritage and the need for preservation of historical structures has led to the continuous development in the past 20 years of a growing number of methods for the analysis of masonry vaults. This notwithstanding some type of vaults, for instance pavilion vaults and fan vaults, despite their broad use in past centuries, have not been thoroughly studied, mainly due to the difficulty of applying simplified theories to their complex shapes. The major simplification that is usually carried out is to reduce the vault to a series of adjacent arches, without transversal connection. Even though simple and accurate, the arch model does not take into account the interaction between the arches and it is not able to properly simulate the three-dimensional effects in the vaults. Although the results are conservative for uniform load distributions, the model limits substantially the set of loading conditions that can be analysed and hence a thorough assessment of vaults performance. This limitation and the need for a flexible method to study the different types of vaults could be solved by using the concept of the surface of thrust within the framework of limit state analysis. The main object of the present paper is the development of a computational procedure which allows to define the 3D structural behaviour of masonry vaults: using limit state analysis with finite friction, the proposed analytical method, based on lower bound approach, allows to obtain, for a generic type of vault, the actual crack pattern, the stress field and the horizontal thrust at the supports for both gravitational and localized loads. In the present paper the limit state analysis with finite friction has been applied to pavilion vaults. The results obtained are compared with non linear F.E. analysis simulations.

1 INTRODUCTION

Computational approaches to the integrity assessment of structural masonry are presently conducted by a variety of methodologies, ranging from highly simplified methods to complex non-linear finite element analyses using plasticity based material models, including joint and interface elements to model planes of weaknesses. Research into modelling of structural masonry has been very active mostly relying on non-linear continuum (Livesley 1978, 1992, Harvey 1988, Melbourne & Gilbert 1994, Hughes 1997) or homogenisation based techniques (Lourenço 1996). While discontinuities can be incorporated by use of smeared crack approach or contact elements, the most reliable solution to date is the use of discrete elements initially developed by Cundall (1971) for rock mechanics and applied to dry block masonry by Amadei (1995), Maunder (1993), Lemos (1997). This approach is particularly useful to analyse cases in which displacement are significant and concentrated at interfaces. The limitation of this technique lies in its high computational burden when meaningful structural models are considered.

Limit analysis has the substantial advantage of disregarding intermediate states of stress in order to identify directly ultimate conditions. It tackles the problem of main interest to structural engineers: control of safety levels. The assumption is that at failure pre-existing self equilibrated states of stress are irrelevant so that direct correlation can be established between external actions and collapse mechanisms.

However these assumptions are only valid for 'standard' materials for which the general theorems of plasticity apply. Due to its lack of ductility and presence of friction, masonry is not 'standard'. The application of classical plasticity is therefore open to criticism. Drucker (1954) shows that the upper limit on collapse loads holds for 'non-standard' materials. Radenkovic (1961, 1962) formulates this result in general terms: existence of a 'standard' instable mechanism proves instability.

On the other hand, the uniqueness of the collapse load disappears. Under some actions and depending

of the existing pre-stresses, a structure may or may not collapse. Sometimes, it is nevertheless possible to find non-null safe limits.

The existence of a safe domain within the friction domain is extended further by Josselin de Jong (1964, 1973) by including the positive influence of normal forces on stability. If through the analysis of the entire structure the value of the minimal normal force acting on the interfaces can be determined, the lower bound safe domain can be extended. Palmer technique can be used to construct it. The limit of applicability of this procedure to masonry structures has been studied by Smars (2000). A prove of uniqueness of the safety factor for vaulted and domed structures under symmetric loading condition, once the magnitude of the normal force is known is given by D'Ayala and Casapulla (2001).

Since Heyman fisrt formulation of the plasticity theorems for masonry (Heyman 1966), limit analysis has been successfully applied to masonry in the 'standard' format under the assumption that the friction coefficient would be high enough to prevent sliding in the range of problems considered. This powerful tool was specifically applied to the safety analysis of masonry arch bridges and later extended to the analysis of vaulted structures; in the search for lower bounds different methods have been used to find admissible state of stresses: funicular methods (Heyman 1966, Harvey 1988, Huerta 2001), membrane analysis (Heyman 1966), network of forces (O'Dwyer 1999), minimum of complementary energy (Maier 1990) or FE with incremental failure analysis.

Livesley (1978, 1992), by adopting a static approach, was the first to developed a formal linear programming procedure to discuss the existence of safe load factor of two-dimensional vaulted structures. Within this approach research has developed substantially in the past decade (D'Ayala 1993, Boothby 1994, Baggio & Trovalusci 1998, Ferris 2001). Friction is often taken into account but the question of applicability of the general theorems of plasticity is not much discussed. If it is usually recognised that the maximum safe load factor can be overestimated, it does not seem to be clear that it is not unique. Only Mauldon et al. (1997) make references to stable, instable and potentially stable domains.

Among masonry structures, arches, vaults and buttresses represent the principal structural component of historic masonry buildings. They epitomise masonry features and problems. They are mainly subjected to compressions, are shaped accordingly and commonly present cracks. Techniques developed for vaults can help to understand and define techniques for other masonry structures.

However the interpretation of masonry vaults' behaviour is difficult, especially when the vaulted surface is not smooth and continuous, leading often to a reduction to an ideal system of many arches. While this oversimplification could be admissible for barrel vaults and spherical domes under simple gravitational loads, cannot do justice of the three-dimensional effects developing in other types of vaults, ribbed or with discontinuity lines. Such effects may be essential to explain stability.

For Heyman (1966), the actual stress state cannot be found. He abandons the behaviour's 'quest' to concentrate on safety. In the spirit of 'standard' limit analysis, all methods able to give an admissible stress state can be used to give a lower bound of the collapse load. Geometry and specific masses are the basic input data. In this approach, the possibility of sliding is ruled out *a priori*. However cracking is considered and resistant mechanisms able to assure the equilibrium after cracking are identified (Heyman, 1977).

The Heyman's study presents a useful and intuitive approach to understand the behaviour of masonry arches and vaults and provides the value of minimum thickness to span ratio as a safe solution under the assumptions of infinite compressive strength and friction resistance and zero tensile strength. Furthermore, this work suggests that, for complex vaults, the junction between two shell surfaces leads to a large stress concentration.

In real vaults however, sliding does occur, especially if accompanied by a loss of shape. In that case, the 'lower bound' estimates can be unsafe. Stereotomy of the vault, coefficient of friction and resistance to tension must then be considered. D'Ayala (1993, 1994, 2001) uses the knowledge of extreme meridian normal forces in a dome to demonstrate its stability, even in the case of potential sliding. Smars (1993, 2000) showed that locally stronger structures are not necessarily safer, proposing a technique to build a lower bound domain for structures having possible local tension resistance.

Nowadays and to our knowledge, no general-purpose software exist permitting 3D limit analysis of vaults. Existing tools are not tailored to their actual behaviour and complex geometry.

In the last years the developments of constitutive laws for masonry structure are been made and most finite element analysis of the masonry vaults are been carried out (Lourenco, 2006).

Nevertheless, the analysis of historical masonry constructions is a complex task and only few proposals specifically oriented to the non-linear analysis of masonry domes and vaults exist.

Oppenheim et al. (1989) propose a limit state analysis of masonry dome, but does not take into account the interaction between the slices.

Nart (2003) describes the mechanical behaviour of masonry domes in relation to the applied loads and geometry. The author's analysis, based on the geometrical parameters, consider a great variety of shapes and

loads, but assume zero hoop stresses and neglect the sliding mechanisms.

Interesting is the work by Block (Block et al. 2006), that propose a structural analysis tools based on the limit state analysis for vaulted masonry buildings. This study extends the graphical method for limit analysis using the line of thrust. Nevertheless it does not provide a complete analysis of three-dimensional behaviour and mechanisms of vaulted structures.

Only few studies explain the tree-dimensional effects. Modelling the principal stresses in a masonry vault as a discrete network of forces, O'Dwyer (1999) develops the limit analysis for vaults, able to take into account redistribution effects. However this work assume an initial value for the horizontal component of the resultant of stresses under the condition that the friction between the voussoirs is sufficient to prevent failure due to sliding.

An iterative procedure for the analysis of the masonry structure, that take into account the non-associative frictional joints, is proposed by Gilbert et al. (2006) that provide a tool for analysing the stability of masonry gravity structures. This method, easy for masonry walls and for rib arches, could be very difficult to apply for three-dimensional structure.

Both the three-dimensional effects and the sliding mechanism are studied by D'Ayala e Casapulla (2001).This study analyzes hemispherical domes by a new analysis tools based on the limit state analysis with finite friction and provides a simple proof of the unique solution.

The same procedure, based on membrane theory with limit state analysis, could be applied at different type of vaults.

Hence, ascertained the value of finite friction in the masonry analysis and the importance of three-dimensional effects for the study to the complex vaults, the paper present a limit state analysis with finite friction applied to a masonry domes, pavilion vaults and fan vaults, in order to evaluate their actual structural behaviour and the minimum thickness to define the stability condition, very important element with regard to structural rehabilitation.

2 STRUCTURAL ASSUMPTIONS FOR MASONRY VAULTS

The structural behaviour of masonry vaults and their collapse mechanisms depends on the material property, so the present theory is founded on the assumption of infinite compressive strength for the blocks, no tension transmitted across the joints and finite friction.

The last hypothesis, often neglected by previous studies, reflects a more realistic masonry mechanical behaviour because, especially for historical structures, after the deterioration of the contact surfaces or of the binding materials, the original friction coefficient could be substantially reduced. Therefore the shear strength at blocks interfaces is not infinite, but determined by the cohesion and the internal friction angle, having assumed the Mohr–Coulomb criterion as a good representation of the real behaviour. Although very little testing has been performed on historic masonry to quantify both characteristic shear strength and friction coefficient, this assumption is supported by work conducted by Hendry et al. (1986) on new masonry assemblies, providing value of friction coefficient lower than 0.4.

Modelling a vault of any shape as a three-dimensional discrete system of rigid blocks, along meridians and parallels, it is possible to determine, by use of the general shell theory, the meridian stresses, the hoop stresses and the shear stresses (Fig. 1). Careful observation of historical vaults and domes highlights that, unless they are corbelled, and independently of the bricks bond (for instance brick courses parallel to the spring, perpendicular to the spring or herringbone brickwork), the joints are always placed in the arch's normal plane, i.e. towards the centre of curvature. Hence, as the weaker elements in the fabric are the joints the analysis can be most usefully carried out at the blocks' interface, where the stress field is related to the frictional (plastic) limits, and where failure by shear or tension will first occur.

While it is evident that the discretization scale could not be representative of each single brick or block constituting the fabric, each portion identified by the intersection of 2 parallels with two adjacent meridians can be considered as a macroelement of homogenous masonry material, with infinite internal compression and tensile and shear strength at the interfaces between portions defined by a Coulomb criterion.

In the case of double curvature vaulted structures, for gravity load distributions, if the material has tensile strength, then membrane theory might be assumed to apply with resultants of meridian and parallel stresses tangent to the middle surface of the vault at any point. As masonry by hypothesis is generally not able to resist tensile stresses for most shapes of vault the gravity load distribution will cause tensile stresses near the spring level that the material is not able to absorb and hence cracks will form. This means that the stress field is modified with respect to the membrane theory, the meridian stress resultant is no more tangent to the meridian geometric curve and generally not centred, so that both resultant bending moment and shear stress resultant are present at the block interface. The curvature of the thrust surface is hence not known a-priori and it is generally not constant.

As a consequence of the accruing of such stress resultants, the equations of equilibrium for classic membrane theory are not sufficient to solve the problem, which has ∞^2 possible solutions. Among those,

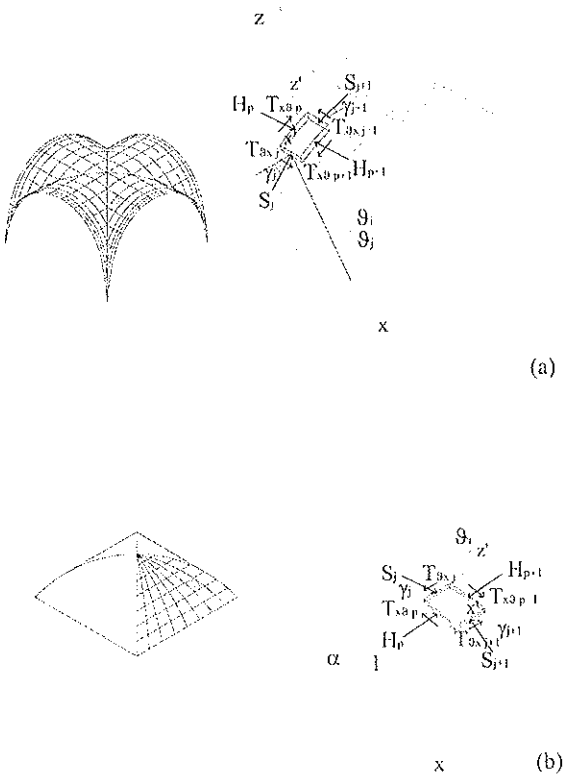

Figure 1. Forces and angles for a generic element of vaults with single curvature; (a) cross vaults, (b) pavilion vaults.

by imposing some condition on material and compatibility, following the theory of plastic limit analysis it is possible to identify the solution that maximise the load-bearing capacity of the vault.

Using the same notation introduced in D'Ayala Casapulla (2001), the first condition, imposed on the material, is the frictional constraints, expressed as:

$$\left|T_j\right| \le T_0 + N_j \mu \tag{1}$$

where:

$$N_j = S_j \cos\left(\vartheta_j - \gamma_j\right) \tag{2}$$

$$T_j = S_j \sin\left(\vartheta_j - \gamma_j\right) \tag{3}$$

As shown in Figure 1 (a,b) , for the generic element of surface j, θ_j is the angle between the vertical and the perpendicular to the elements's surface (z' in the local system) and γ_j is the angle that the resultant of stress S_j along the arch forms with the horizontal axis at each interface. Hence N_j and T_j are the components of S_j normal and parallel to the interface, respectively.

Equation (1) identifies the maximum and the minimum value of the shear resultant and identifies the

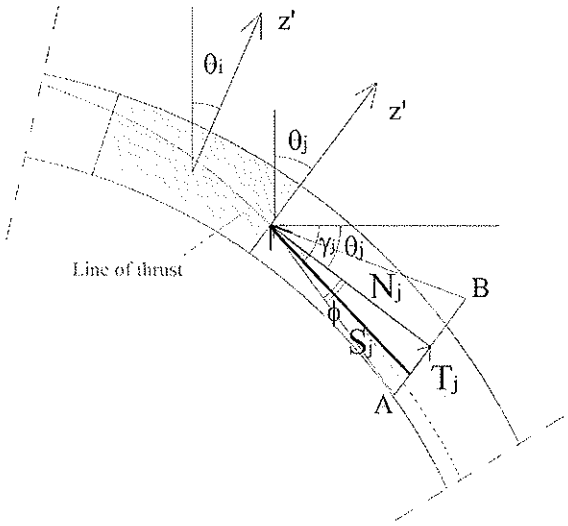

Figure 2. Oversimplification of forces Nj and Tj, components of Sj normal and parallel to the interface J respectively, and Coulomb's cone projection.

points A and B on the Coulomb's cone projection (Fig. 2). If the tangential force T exceeds the limit, the vault could fail by way of sliding. This means that, in case of symmetric loading, there is a unique limiting value of the shear force, and the local equilibrium problem is at a limit state statically determined.

Imposing the equilibrium condition and applying the lower bound static analysis, it is possible to identify a unique solution of the problem, from which the line of thrusts can be derived and the minimum thickness quantified.

In the present paper the previous approach is extended by relaxing the condition of axial symmetry used for domes. A lower bound approach is developed for pavilion vaults, where the state of stress and hence the shear resultant are variable from meridian to meridian, and where singular conditions develop along the diagonal as the intersection of two webs is not smooth. It will be shown that by using optimisation techniques is possible to fully define the state of stress, the maximum capacity and the required thickness at collapse. The results are compared with a non linear finite element analysis of the same vault.

3 LOWER BOUND APPROACH WITH FINITE FRICTION

Masonry pavilion vaults, despite their common use in past centuries, in particular in XVI–XVII century palaces, have not been studied in any greater depth yet, principally because due to their singularity of shape and presence of cuspide form along the diagonal, the

complex 3-dimensinal state of stress that develops in presence of uniform gravity loading does not lend itself easily to simplified approaches.

These vaults have continuous support along walls; have finite curvature in the direction of the meridians, but infinite curvature along horizontal plane. This means that there can be no contribution to recentre the line of thrust from hoop stresses and hence membrane theory is inherently non applicable. This means that such type of vaults is often affected by cracks along the diagonals, where the geometry of the vault is farthest from the geometry of the thrust surface generated from the gravity load distribution. Cracks can also appear toward the centre of the web of each portion so, in the past, they are been often modeled as independent arches.

However the simplified arch model, does not account for the capacity of the vault to transfer load associated with shear and for the arch effect that can be develop within the horizontal strips due to their non negligible thickness, similarly to the arch effect accounted for in walls or slabs.

On the basis of this considerations and suitably simulating the boundary conditions and the condition of equilibrium that arise along the diagonal due to the singularity of the surfaces along the diagonals, limit state analysis can be applied to this family of vaults to determine their state of stress at failure.

The main objective of the present section is to understand, through the limit state analysis approach, the structural behaviour of pavilion vaults, in order to evaluate with more accuracy the actual stress field that can cause cracks.

Moreover this method allows finding the thrust line position and the admissible thrust surfaces, leading to the calculation of the minimum thickness which satisfies at the same time equilibrium and compatibility. This is of great importance with regard to strengthening interventions because it allows determining the vaults' safety factor, which can be expressed, as proposed by Heyman as the ratio between the geometric thickness over the minimum required thickness, but also the accurate position of the hinges at failure and hence the appropriate positioning of ties or other thrust contrasting devices.

The simplest case to analyse is a pavilion vault over a plane square area and of semicircular curvature, which is also the most frequent occurrence according to the technical literature (Scamozzi, 1615), subject to self weight loading.

Figure 3 shows the geometric characteristic of the vault's generatrix, where R is its radius, f is the vault's rise, l is the span. In the numerical procedure the slices that make up half of the web between to successive ribs are considered, these being present only along diagonal. The ribs according to historic the technical literature, as shown in figure 3, can be described by

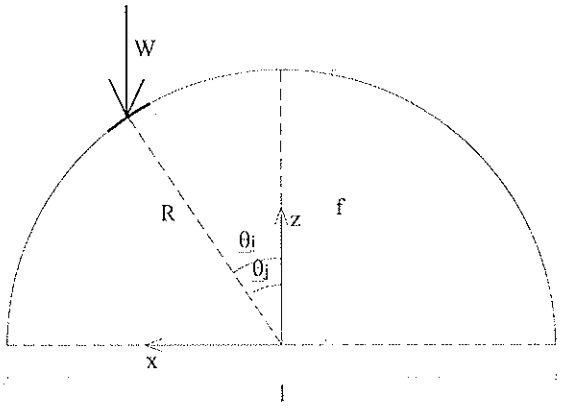

Figure 3. Geometric characteristics of the vault's generatrix.

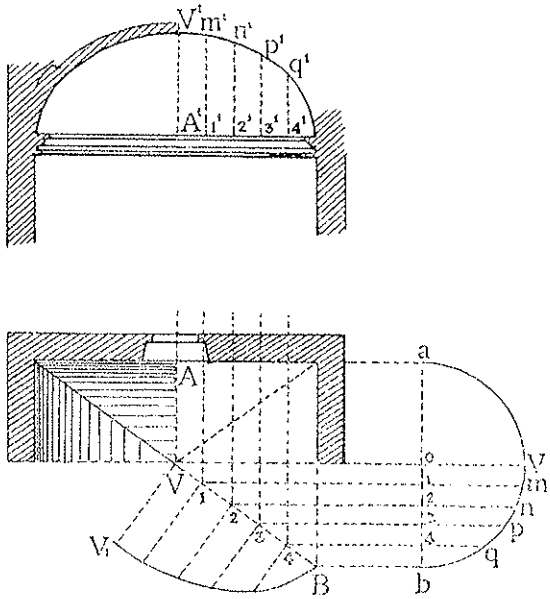

Figure 4. Geometric characteristic of the diagonal and of the vault's generatrix, used for the centring work (Levi, 1932).

the equation of an ellipsis (Curioni, 1870; Breymann, 1885; Levi, 1932).

Assuming the n slices are made up of m blocks, each block is identified, in the global system, by the coordinates of its centre of mass:

$$x_i^{geom} = R \cdot sen\underline{\vartheta_i} \tag{4}$$

$$z_i^{geom} = R \cdot \cos\underline{\vartheta_i} \tag{5}$$

$$y_i^{geom} = R \cdot sen\underline{\vartheta_i} \tan\alpha_k \tag{6}$$

for i = 1 to m and k = 1 to n
were α_k is the horizontal angle between the x axis in the global system and the horizontal projection of x-axis in the local system as shown in Figure 5 and $\underline{\theta_i}$

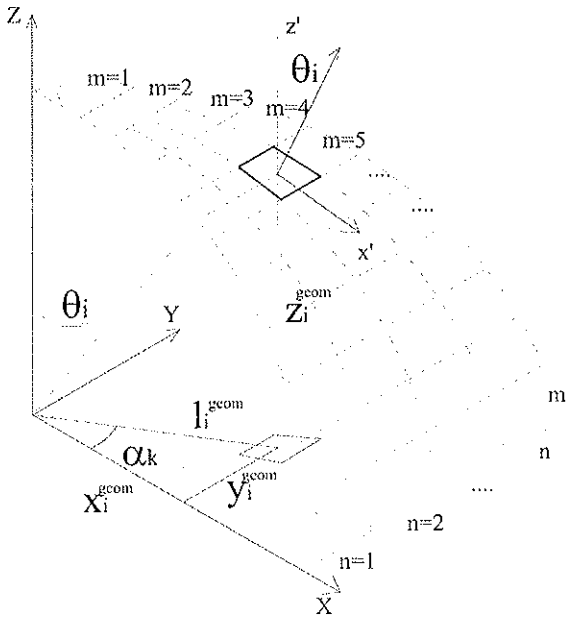

Figure 5. Generic block with the coordinates of its centre of mass and the angles α_k, $\underline{\vartheta_i}$ and $\underline{\vartheta_i}$.

is the angle between the vertical and the perpendicular to the generatrix. The relation between ϑ_i and $\underline{\vartheta_i}$ is:

$$\tan \underline{\vartheta_i} = \tan \vartheta_i \cdot \cos \alpha_k \tag{7}$$

The state of stress for each slice's element is completely defined by equilibrium equations and the resultant of stresses depends on the position of z_i.

The z_i coordinates are assumed as geometric unknowns and the position of the thrust surface is found by means of a discrete approach through the calculation of its coordinates, hence:

$$x_i^t = x_i^{geom} \;,\; y_i^t = y_i^{geom} \;,\; z_i^t = z_i \tag{8}$$

The distance between the origin of the axes and each point of the thrust surface is:

$$R_i^t = \sqrt{\left(l_i^{geom}\right)^2 + \left(z_i^t\right)^2} = \sqrt{\left(\frac{x^{geom}}{\cos \alpha_k}\right)^2 + \left(z_i^t\right)^2} \tag{9}$$

where l_i^{geom} is the horizontal projection of the distance between the block's centre of mass and the origin of the global system.

The distance between the origin of the axes and each point of the middle surface is:

$$R_i^{geom} = \sqrt{\left(\frac{x_i^{geom}}{\cos \alpha_k}\right)^2 + \left(z_i^{geom}\right)^2} \tag{10}$$

Hence, the eccentricity of the thrust surface at each point is:

$$e = \Delta R = \left| R_i^{geom} - R_i^t \right| \tag{11}$$

and the minimum constant thickness t required is:

$$t = 2 \max \Delta R \tag{12}$$

This can be the objective function to minimise.

The meridian, hoop and shear stresses are calculated considering the coordinates of the generic surface of thrust at the interface between blocks. Subsequently, by limiting the maximum values of the internal shear force T_j, component of S_j parallel to the interface, which can not be greater than the frictional strength at each block interface, the thrust surface's z_i coordinates that satisfy the material constraints are determined.

The coordinates of the generic thrust surface at the interface are:

$$z_j^t = \frac{z_i^t + x_i^t \cdot \tan \gamma_j}{1 + \dfrac{\tan \underline{\vartheta_j}}{\cos \alpha_k} \cdot \tan \gamma_j} \tag{13}$$

$$x_j^t = z_j^t \cdot \tan \underline{\vartheta_j} \quad \text{and} \quad y_j^t = R_i^t \cdot sen \underline{\vartheta_j} \tan \alpha_k \tag{14}$$

$$l_j^t = z_j^t \cdot \frac{\tan \underline{\vartheta_j}}{\cos \alpha_k} \tag{15}$$

In equation (13) γ_j is the angle that the resultant of stress S_j along the meridian forms with the horizontal axis at each interface and it is defined as:

$$\gamma_j = \arctan \left| \frac{z_{i+1}^t - z_i^t}{l_{i+1}^t - l_i^t} \right| \tag{16}$$

Hence, simplifying and neglecting the second order terms, with regard to a slice element, the equilibrium along the local z axis yields the meridian force S_j:

$$S_j = \frac{-W \cdot \cos \gamma_i}{sen\left(\gamma_i - \gamma_j\right) + sen\left(\gamma_{j+1} - \gamma_i\right)} \tag{17}$$

In (17), having defined ω the weight for unit surface and n the number of meridian slices (see figure 5), the weight W_j of the portion of each block identified by angles ϑ_j and ϑ_{j+1}, is:

$$W_j = \frac{\omega R^2 \left(1 - \cos \underline{\vartheta_{j+1}}\right)}{n} - \frac{\omega R^2 \left(1 - \cos \underline{\vartheta_j}\right)}{n} \tag{18}$$

where γ_i is the angle that the tangent of the thrust line at the centre of each element forms with the horizontal axis.

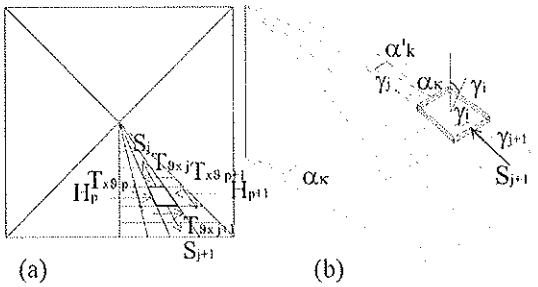

Figure 6. (a) view from the top of the pavilion vault, with the forces for a generic element, (b) axonometric showing the angles γ_i and α'_k.

The shear force at the interface between two slices, shown in Figure 6a, can be quantified using translation equilibrium:

$$T_{x\vartheta\, p+1} = S_j \cdot \cos(\gamma_i - \gamma_j)_k - S_{j+1} \cdot \cos(\gamma_{j+1} - \gamma_i) - W \cdot sen\gamma_i + T_{x\vartheta\, p} \tag{19}$$

where the subscript p indicates the lateral surface of the generic block.

Given the symmetry of the problem, for the interface between the slices at the centre of the web, corresponding to $p = 0$, the shear resultant $T_{x\vartheta} = 0$.

Hence, using rotation equilibrium around an axis normal to the surface, the shear resultant $T_{\vartheta x}$ at any location is:

$$T_{\vartheta x\, j+1} = \frac{\left(T_{x\vartheta\, p} + T_{x\vartheta\, p+1}\right) \cdot \cos\alpha'_k \cdot sen\vartheta_j \cdot \left(tg\alpha_{p+1} - tg\alpha_p\right)}{\vartheta_{j+1} - \vartheta_j} - T_{\vartheta x\, j} \tag{20}$$

where the angle α'_k is the angle α_k projected in the plane tangent to the thrust surface at the centre of element (Fig. 6b):

$$\alpha'_k = sen^{-1}\left(\cos\gamma_j \cdot sen\alpha_k\right) \tag{21}$$

For $j = 0$ the shear force $T_{\vartheta x} = 0$.

The horizontal force H_p can be determined imposing the boundary condition along the diagonal and considering half web.

The shear force $T^d_{x\vartheta}$, corresponding to shear force $T_{x\vartheta}$ along the diagonal, can be determined by considerations of global equilibrium:

$$\Sigma(T^d_{x\vartheta} \cdot sen\gamma_i) = -W_{tot} - S_j \cdot sen\gamma_j \tag{22}$$

Starting from $i = 1$, for a generic block m along the diagonal, identified by the surfaces $j - 1$ and j, the shear force $T^d_{x\vartheta}$ calculated at its centre i is:

$$T^d_{x\vartheta} = \frac{-W_{tot} - S_j \cdot sen\gamma_j - \sum_{i=1}^{m-1}(T^d_{x\vartheta} \cdot sen\gamma_i)}{sen\gamma_i} \tag{23}$$

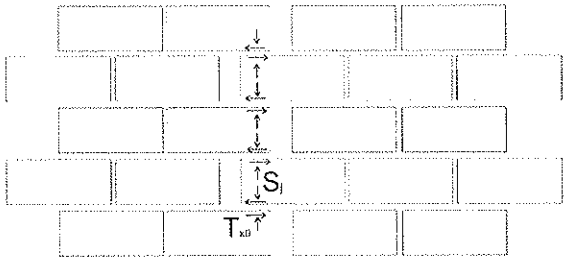

Figure 7. Cracked masonry showing the shear force $T_{x\vartheta}$ and the force S_j transmitted between the blocks.

Hence the horizontal force H_p along the diagonal is:

$$H_p = T^d_{x\vartheta} \cdot sen\alpha'_{k=\pi/4} \tag{24}$$

Starting from the diagonal slice, for horizontal equilibrium, the parallel force H_{p-1} is:

$$H_{p-1} = H_p - T_{\vartheta x\, j} + T_{\vartheta x\, j+1} - S_j sen\alpha'_k + S_{j+1} sen\alpha'_k - T_{x\vartheta\, p} \cdot sen\alpha'_k + T_{x\vartheta\, p+1} \cdot sen\alpha'_k \tag{25}$$

If H_p exceeds the tensile strength of material (by assumption equal to zero), the hoop stresses are not present and the horizontal equilibrium equation reduces to:

$$T_{\vartheta x\, j} + S_j sen\alpha'_k + T_{x\vartheta\, p} \cdot sen\alpha' = T_{\vartheta x\, j+1} + S_{j+1} sen\alpha'_k + T_{x\vartheta\, p+1} \cdot sen\alpha'_k \tag{26}$$

For equilibrium to rotation around an axis normal to the element surface a resultant shear force $T_{x\vartheta}$ is present due to the brick staggering (see Fig. 7) and its components along the S direction at the j and $j + 1$ interfaces are the same.

Hence the meridian resultant S after cracking becomes:

$$S^* = \sqrt{\left(S_{j-1}\cos\alpha'_k \cos\gamma_j\right)^2 + \left(S_{j-1}\cos\alpha'_k\, sen\gamma_j + W\right)^2} \tag{27}$$

And the corresponding angle γ^* is equal to:

$$\gamma^* = -tg^{-1}\frac{S_{j-1} sen\gamma_{j-1} + W}{S_{j-1}\cos\gamma_{j-1}} \tag{28}$$

Both the normal and shear resultant at this interface can be obtained as components of S^* as follows:

$$N_j = S^* \cdot \cos(\vartheta_j - \gamma^*_j) \tag{29}$$

$$T_j = S^* \cdot sen(\vartheta_j - \gamma^*_j) \tag{30}$$

Imposing the frictional constraint:

$$|T_j| \leq T_0 + N_j \mu \tag{31}$$

The optimum programming problem is completely defined if the maximum eccentricity of the thrust surface is minimized as shown in (11). Conditions (35) together with the target function (11) or (12) completely define the physical state of the vault and its mechanism of collapse, as the values of the indexes i and j for which the = sign applies in (11) and/or (35) identifies the cross sections along the arch for which either rotation or sliding are about to occur.

Furthermore the problem set in these terms can be easily extended to generic conditions of loading and constraints as the symmetry is only invoked to define an initial value of shear resultant at midspan, but this can easily be obtained by using generic global equilibrium considerations.

4 RESULTS FOR SQUARE PAVILION VAULTS

The limit state analysis with finite friction constitutes a new tool to define the 3D structural behaviour of masonry vaults. By means of an easy and rigorous procedure, developed with commercial programs (for example Excel), it is possible to obtain an optimum solution considering the load redistribution after cracking.

Identifying the optimal thrust surface, the proposed analytical method, based on lower bound approach, allows determining, for any vaults, some important elements with regard to safety assessment and needs for intervention, such as:

- the masonry vaults' safety factor, expressed as the ratio between the actual thickness over the minimum thickness required by (12);
- the resultant tensile forces in the parallel direction and hence the actual crack pattern (equation 28);
- the complete resultant stress field and the thrust surface's eccentricity;
- the resultant shear force at blocks interfaces;
- the horizontal thrust at the supports.

Furthermore, this approach is able to provide in very modest time the same results obtained by means of nonlinear FEA analyses, often too laborious because of their high computational burden and the difficulty in interpretation of the results.

To demonstrate the effectiveness of the procedure and to clarify the role of interaction between arches in complex vaults, the results on pavilion vaults are discussed in this section and the comparison with a FE model will be shown in the following one.

Considering a pavilion vault with generatrix radius R equal to 3 m, vault's rise f equal to 3 m and span l equal to 6 m, the results are presented for the slices that make up half of the web between to successive ribs. Figure 8 shows the four slices that compose arbitrarily the portion of vaults considered.

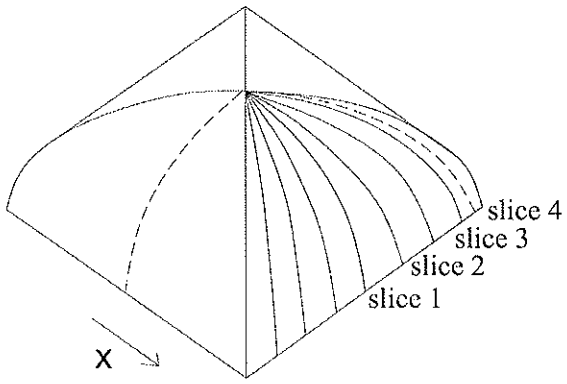

Figure 8. Division of an half web in slices and nomenclature for the procedure.

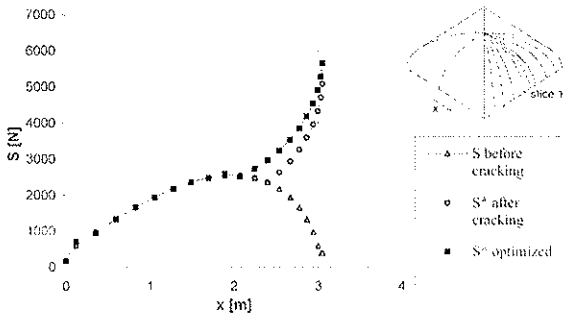

Figure 9. Meridian force S before cracking, after cracking and after the optimization for the central slice.

4.1 *Meridian force S*

After cracking the meridian stress resultant is no more tangent to the meridian geometric curve and generally not centred. Figures 9 and 10 illustrate the variation of meridian force S with respect to the horizontal coordinate x, in absence of cracking, after cracking has occurred and after cracking and running the optimization procedure to obtain the minimum eccentricity, for slices 1 and 4. The chart show that the resultant S, before cracking, increase up to 2 m, corresponding to $\underline{\theta} = 45°$, and reduce in the final portion of the slice. This solution corresponds to the membrane solution that might occur if the material has tensile capacity. Since the masonry is generally not able to resist tensile stresses, near the spring the cracks along the meridian direction will form and the force S* departs from S along the cracked surface.

Figures 9 and 10 also show the force S* obtained minimizing the maximum thrust surface's eccentricity

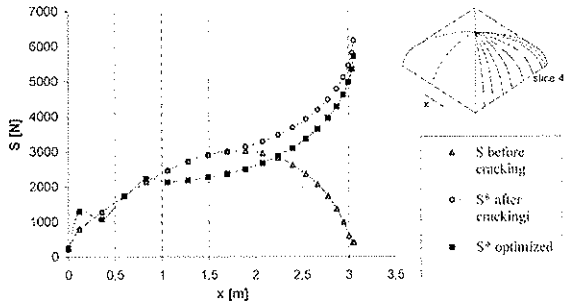

Figure 10. Meridian force S before cracking, after cracking and after the optimization for the slice near to diagonal.

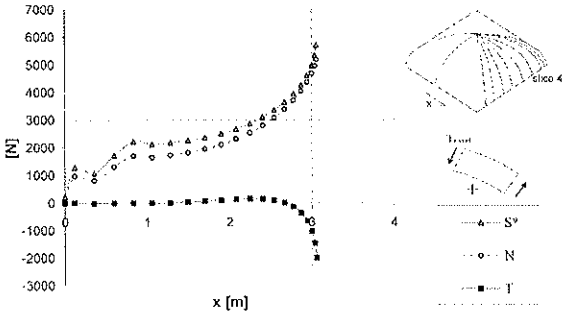

Figure 12. S*, normal force N and shear force T at the interface for the slice near to diagonal.

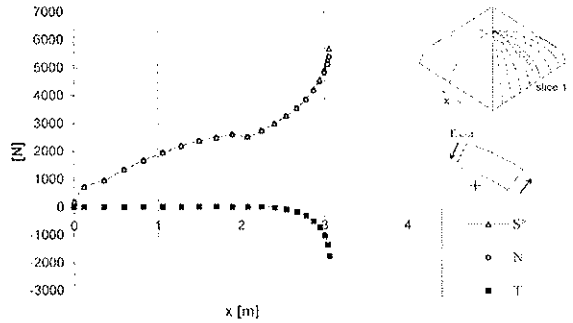

Figure 11. S*, normal force N and shear force T at the interface for the central slice.

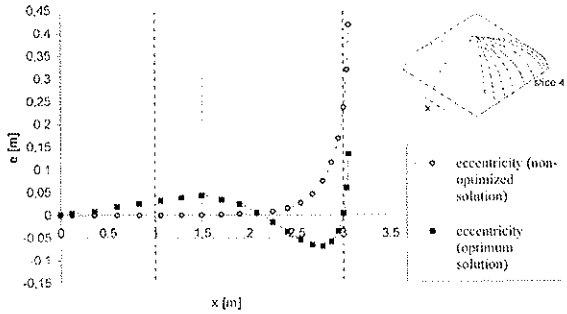

Figure 13. Thrust surface's eccentricity for the non-optimized solution and for the optimum solution (slice near to diagonal).

and imposing the material constrains. This force presents the same trend of the S* before optimization, but the optimum S* diverges earlier from the membrane solution, indicating that cracks will extend further in along the meridian but that the value of the resultant is smaller. This change in value id directly related to the distribution of eccentricity, especially for the slice closer to the diagonal as it will be seen in 4.3.

4.2 *Normal force N and shear force T at the interface*

The resultant meridian normal force N and shear force T at the interface, components of S* normal and parallel to the interface respectively, are shown in Figures 11 and 12. As it can be seen, the force N shows the same trend of S* while the shear force T is equal to zero up to the cracking point, where the thrust line is perpendicular to the block interface, and it increases in the cracking area, where the funicular breaks away from the middle surface because of the absence of axial forces along the parallel. Besides, it can be observed that, from the centre of the web to the diagonal, the shear force T increase. Indeed the angle γ_j, representing the inclination of the thrust line, increasingly differs from the geometric angle θ_j moving from the centre of the web to the diagonal.

4.3 *Thrust surface's eccentricity*

The thrust surface's eccentricity is shown in Figure 13. It should be noted that the non-optimized solution differs everywhere from the optimum solution. The non optimized solution, indeed, is equal to zero along the uncracked area and it has an exponential trend from the haunches to the support, because the absence of the hoop stresses requires an infinite thickness.

It is well known that, with a lower bound approach, between the ∞ possible solutions, the actual solution is the one that maximise the load-bearing capacity of the vault while the thrust surface is constrained within the vault's thickness: imposing the condition of minimum eccentricity and the condition that the friction between the voussoir is sufficient to prevent failure due to sliding, the actual solution can be identified. Hence, as shown in Figure 13, the eccentricity in the optimum solution reduces drastically and the presence of relative peaks indicate the possible formation of plastic hinges at the extrados, at x equal to 1.5 m ($\underline{\theta_j} = 30°$), and at the intrados, about at x equal to 2.78 m ($\underline{\theta_j} = 65°$). The eccentricity presents its absolute maximum at the support.

The chart in Figure 14 shows the corresponding bending moment for the four slices, calculated as the product of the meridian normal force N and the

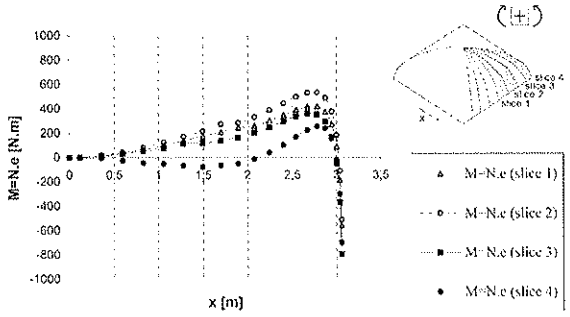

Figure 14. Bending moment for all the slices belonging to half web.

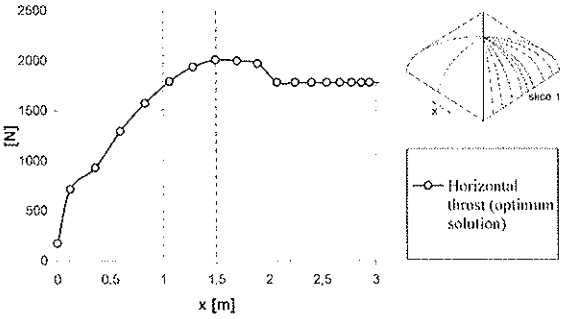

Figure 15. Horizontal component of S* along the meridian in the web centre.

eccentricity. The maximum bending moments for all slices are localized at the support confirming the presence of extrados plastic hinges there.

4.4 *Horizontal thrust at the supports*

The possible intradox plastic hinge at x equal to 2.78 m and usually the presence of a spandrel wall that contribute to increase the thickness in the portion of the vault near the support, has the effect of identifying only the portion contained between an aperture of the subtending angle of 2 θj as the actual portion of structure behaving as a vault, the lower part being usually considered as solid with the supporting walls. This in turn means that the critical cross section along the meridian where the horizontal thrust should be assessed is at $\theta j = 65°$, according to the previous results.

Furthermore, as it can be seen in Figure 15, showing the horizontal component of S* along the meridian at the centre of the web, the horizontal thrust is constant in the cracked portion, where the hoop stresses are not present.

The values of the horizontal thrust however is also directly influenced by the lateral stiffness of the perimeter walls supporting the vault: depending on the effective slenderness of the walls and their connection to the vault, they will have a direct effect on restraining lateral movement of the vault and hence on the value of the thrust developed within it. The limit conditions of roller support and full fixity are both unlikely to be met I practice. For the purpose of the procedure the supports are considered as fixed, and this will provide an upper limit of the value of the thrust. The value of horizontal thrust is very important in a strengthening intervention because allows to determine the ties position and strength.

Figure 16 shows the variation of horizontal thrust along the support parallel, for half of the web length before and after the optimization. It should be noted that the first solution corresponds to considering each slice independently and yields a minimum value at the centre of the web were the ratio of rise over span is higher. After the optimization redistribution occurs

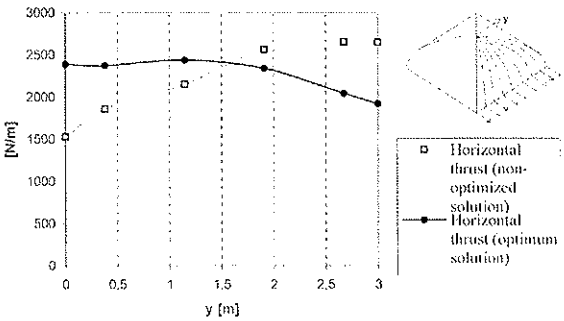

Figure 16. Horizontal thrust for the non-optimum solution and for the solution after the optimization.

via shear and arch effect at parallel level yielding the opposite results with a trend slightly decreasing from the centre to the diagonal.

5 COMPARISON WITH FINITE ELEMENT MODEL

The validation of the proposed approach based on the limit state analysis is carried out by comparing the results in terms of stress resultants with the output obtained by advanced non linear FE modelling.

The Finite Element Model has been constructed using the *Algor V19* FE program: shell elements are used for all uncracked masonry portions and contact elements are inserted at the interface between shell elements where tensile stress develops.

The following material properties have been assumed: specific weight $\gamma = 1850\,\text{kg/m}^3$; Poisson's ratio $\nu = 0.15$; Elastic Modulus E = 5000 MPa.

For an easier comparison between the results of the limit state analysis and the FE analysis, the FE mesh has half the size of the limit state analysis along the parallel but the same number of subdivisions along the meridian, (Fig. 17).

To simulate the presence of perimeter walls high 3 m and thick 0.50 m, Shell elements are been arranged

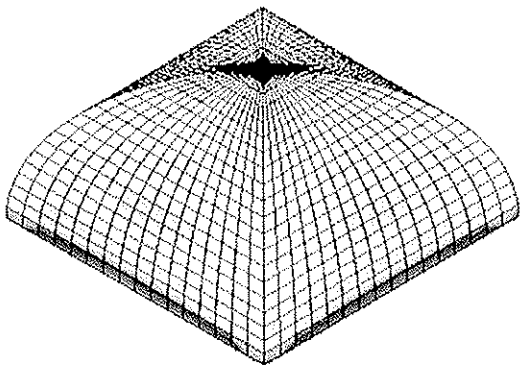

Figure 17. Axonometric showing the Finite Elements model of the pavilion vault.

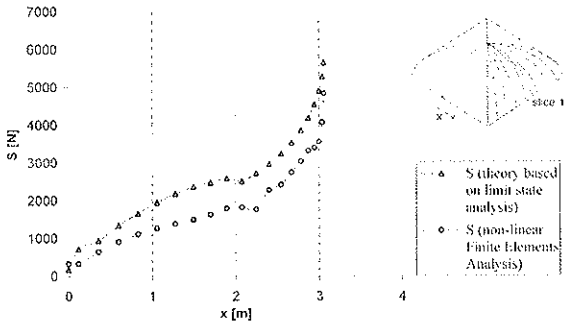

Figure 18. Comparison between the meridian forces S obtained by the limit state analysis and the Finite Elements Analysis along the central slice.

along the supports and they are constrained by fixed nodal boundary conditions at the abutments.

Figures 18 and 19 show the comparison between the meridian forces S obtained by the optimised limit state analysis and the Finite Elements Models along the central slice and along the slice near to diagonal respectively. Both curves present the same trend, characterized by a change of curvature in the cracking area, this means that the new theory based on limit state analysis with finite friction accurately predicts the behaviour of pavilion vaults, identifying the actual crack pattern and the meridian resultant S field. As it can be seen, in agreement with the safety theorem of limit state analysis associated with lower bound approaches, the values of S as calculated by the procedure are always slightly greater than the actual state of stress identified by the FE analysis.

Also the normal force N and shear force T have the same trend in the two models.

Furthermore, the eccentricity and hence the position of the thrust surface is accurately calculated with

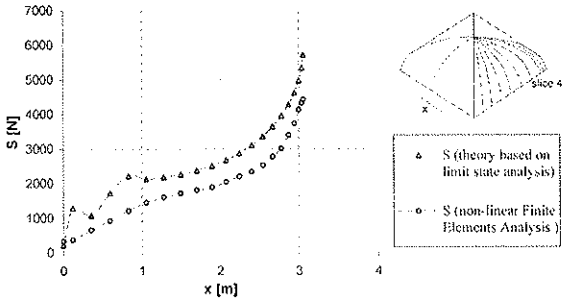

Figure 19. Comparison between the meridian forces S obtained by the limit state analysis and the Finite Elements Analysis along the slice near the diagonal.

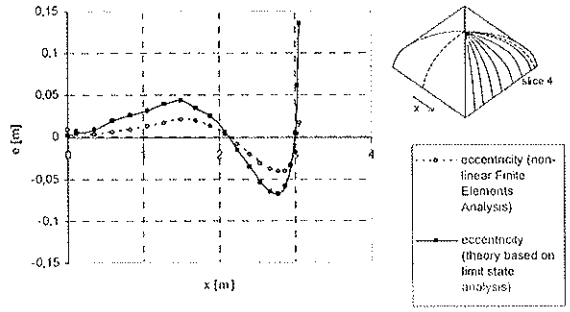

Figure 20. Comparison between the eccentricities obtained by the limit state analysis and the Finite Elements Analysis along the slice near the diagonal.

the limit state analysis. As it can be seen, again in favour of safety, the values computed by the procedure are slightly greater than the values obtained with the FE, however the location of relative minimum and maximum and absolute values identify with great accuracy the actual position of plastic hinges along the slices.

The identification of the position of the extrados hinge is particularly critical, as this also define the position along the arch of the maximum horizontal thrust and hence is essential for the correct positioning of ties or for the construction of abutments.

Values of horizontal thrust have been compared for the two analyses for and angle $\theta = 65$ degrees and for the condition of full lateral restraint at the support for the F.E. model.

As it can be observed in Figure 21 where the thrust is plotted along a half parallel between midspan ($y = 0$) and the diagonal, the trend is again similar in the two cases with the values estimated by the procedure being clearly equal to the F.E at midspan and slightly overestimated as progresses toward the diagonal with a maximum difference of 20% .

Hence it is possible to affirm that the new theory is able to provide the actual crack pattern and the stresses field in the masonry vaults.

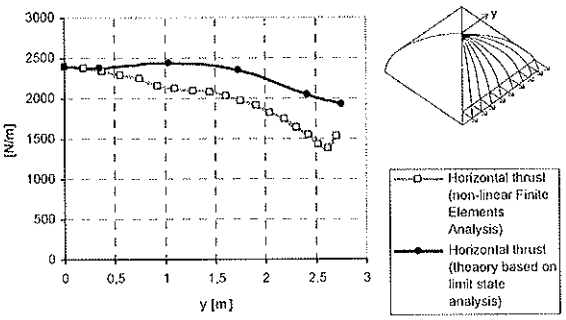

Figure 21. Comparison between the horizontal thrust obtained by the limit state analysis and the Finite Elements Analysis.

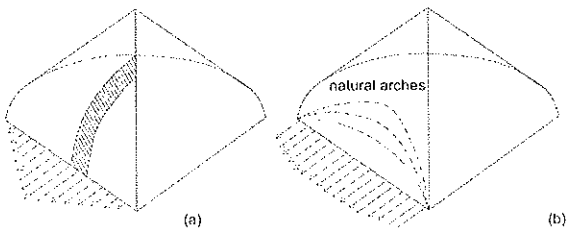

Figure 22. Horizontal thrust along the supports obtained by the simplified arch model (a) and the actual horizontal thrust obtained by the limit state analysis (b).

6 DISCUSSION OF RESULTS

The limit state analysis with finite friction and the FE analyses have allowed to clarify some important aspects of the complex structural behavior of pavilion vaults, in particular concerning the three-dimensional effects and the importance of the sliding. The results on pavilion vaults demonstrate that also vaults with rigid boundary at the supports are affected by cracks along the diagonals, unlike the common opinion that ascribes the diagonal cracks only to the walls' overturning.

In addition the structural behavior of masonry pavilion vaults can not be reduced to a series of adjacent arches, without transversal connection. In fact, in the web, despite the cracks along the diagonals, any arch can transfers the stresses at the arches beside it. This interaction is clear observing the trend of horizontal thrust applied by the vaults on the walls (Fig. 22): as it can be seen, the actual horizontal thrust is about constant, differently from the few indications about the pavilion vaults reported in the scientific literature, which indicates a triangular trend resulting from the simplified arch model.

This means that the web develops a series of natural arches defining an alternative load path from the centre of the web to the diagonal.

The theory based on the limit state analysis also allows to identify the thrust surface and to evaluate the bending moments for any slice. The results

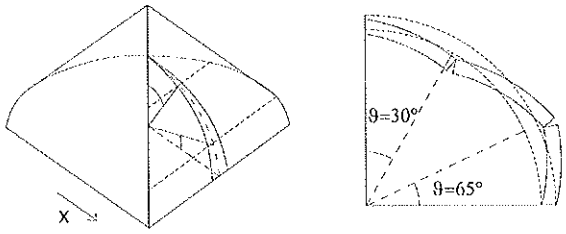

Figure 23. Possible vault's collapse mechanism for any slices.

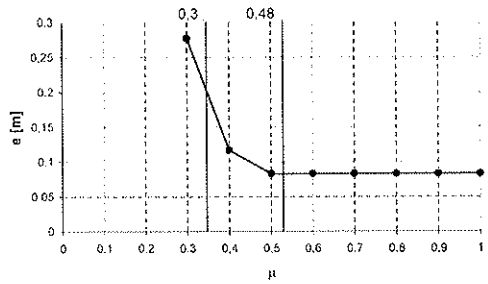

Figure 24. Maximum thrust surface's eccentricity obtained by the limit state analysis with finite friction for different friction coefficients μ.

show that two plastic hinges might form: the first one located at the extrados, for x equal to 1.5 m ($\theta_j = 30°$), and the second one at the intrados, for x equal to 2.78 m ($\theta_j = 65°$). Figure 24 shows the likely collapse mechanism.

In addition, the vault could fail by way of sliding. Using the limit state analysis with finite friction it is possible to evaluate the minimum thickness which satisfies at the same time equilibrium and compatibility. The application of this new theory on pavilion vaults shows that, for a friction coefficient higher than 0.48, the shear force T are everywhere smaller than N. μ, hence the results are unrelated to the friction coefficient and sliding mechanism are prevented.

On the other hand, in the 0.3–0.48 friction coefficient range, the vault is able to find a new equilibrium system, in which the stress resultants are unvaried, but the eccentricity considerably increases (Fig. 24). This means that the thickness necessary for the vault's stability would increase and consequently the safety factor decrease. It is necessary to specify that the maximum eccentricity is located near the support, where typically the spandrel ensures a big thickness.

For friction coefficient lower than 0.3 the Excel's solver cannot find a feasible solution, i.e. it cannot satisfy all constraints.

Moreover, the structural behaviour of masonry vaults could vary with the rise-span ratio f/l. As pointed out by Palladio (1570) and Guarini (1737), the most frequent geometry in XVI-XVII century palaces would typically results in f/l ratios equal to 1/3, 1/4 and

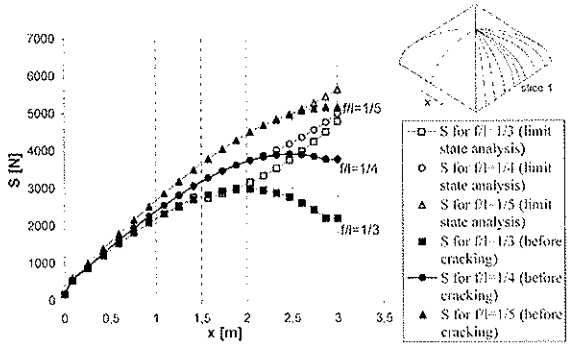

Figure 25. Comparison between the meridian forces S obtained by the limit state analysis after meridian cracking and before meridian cracking for the rise-span ratio equal to 1/3 (rise = 2 m), 1,5 (rise = 1,5 m) and 1,2 (rise = 1,2 m) respectively (central slice).

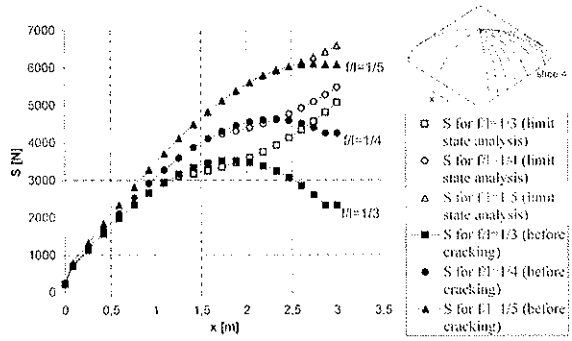

Figure 26. Comparison between the meridian forces S obtained by the limit state analysis after meridian cracking and before meridian cracking for the rise-span ratio equal to 1/3 (rise = 2 m), 1,5 (rise = 1,5 m) and 1,2 (rise = 1,2 m) respectively (slice near to the diagonal).

1/5. Figures 25 and 26 show the comparison between the meridian forces S obtained with the limit state analysis after cracking and before cracking for pavilion vaults over a plane square area, of semicircular curvature and of rise equal to 2 m (f/l = 1/3), to 1,5 m (f/l = 1/4) and to 1,2 m (f/l = 1/5) respectively. As it can be observed, the force S increase with decreasing rise-span ratio, nevertheless, decreasing the rise, the classical membrane solution, that represents the stress field before meridian cracking, converges on the optimum solution. In fact, reducing the f/l ratio, also the eccentricity's trend is towards zero (Fig. 27) and the tensile area near to the spring decreases (Fig. 27); this means that, in shallow vaults, the geometry is closer to the thrust surface generated by the gravity load distribution, and compression hoop stresses H_p are present for a grater portion of the surface (Fig. 28). This means that the spread of the cracks that often develops along the diagonal and in the centre of the web depends on the vault's rise and hence, for f/l ratio smaller than about

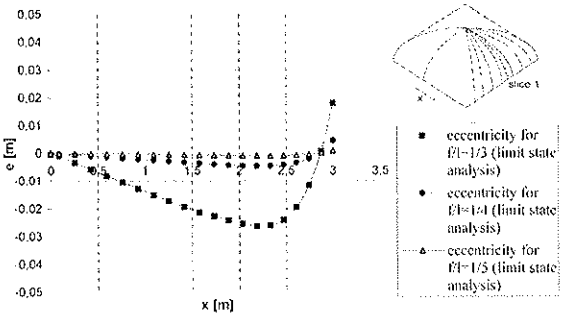

Figure 27. Comparison between the eccentricities obtained by the limit state analysis for the rise-span ratio equal to 1/3 (rise = 2 m), 1,5 (rise = 1,5 m) and 1,2 (rise = 1,2 m) respectively (central slice).

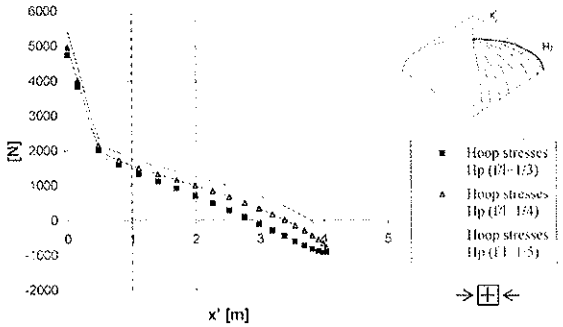

Figure 28. Comparison between the hoop stresses H_p obtained by the limit state analysis for pavilion vaults with a rise-span ratio equal to 1/3 (rise = 2 m), 1,5 (rise = 1,5 m) and 1,2 (rise = 1,2 m).

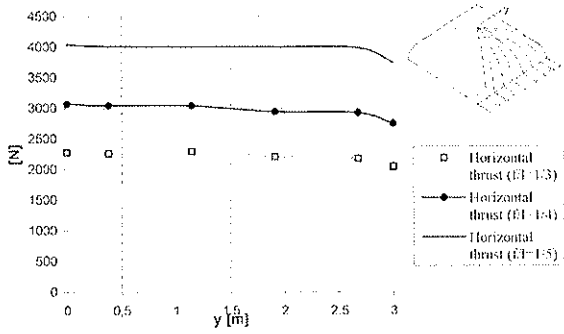

Figure 29. Comparison between horizontal thrust along the supports obtained by the limit state analysis for pavilion vaults with a rise-span ratio equal to 1/3 (rise = 2 m), 1,5 (rise = 1,5 m) and 1,2 (rise = 1,2 m).

1/5, the classical membrane theory could be used with good approximation.

As it is well known, the horizontal thrust increase if the vault's rise reduces; furthermore it is possible to observe that its trend along the perimeter walls tends to become constant for shallower vaults (Fig. 29). This means that, reducing the rise/span ratio, the natural

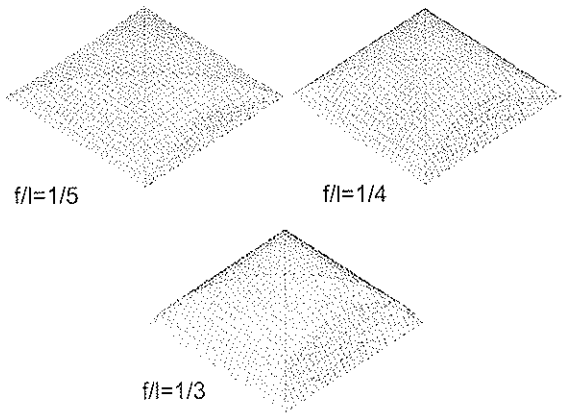

Figure 30. Qualitative developments of natural arches for pavilion vaults with a rise-span ratio equal to 1/3 (rise = 2 m), 1/5 (rise = 1.5 m) and 1/2 (rise = 1,2 m).

arches, that develop in the pavilion vaults and that cause the transfer of meridian stresses from the centre of the web to the diagonal, affect a smaller area near to the diagonal, as it can been see from the qualitative pictures in Figure 30.

7 CONCLUSIONS

The paper presents a new 3D limit state analysis for vaulted structures, based on finite friction, able to describe the actual structural behaviour of a wide range of masonry vaults. Assuming finite friction between block interface and using a lower bound approach, this theory allows the identification of the optimal thrust surface, so it is possible to define, for a generic type of vaults, the actual crack pattern and the stress field. The development of a computer procedure is of great importance with regard to strengthening interventions because it allows determining easily the masonry vaults' safety factor, given by the actual thickness over the minimum thickness ratio, to understand the cause of the cracks and to find the horizontal thrust on the supports.

In addition, the limit state analysis with finite friction allows investigating aspect previously neglected.

In particular, while it is recognized that often masonry vaulted structures fails by way of sliding, most of existing analysis on masonry vaults don't consider the limited friction. However the use of friction limits is particularly valuable because, after the deterioration of the contact surfaces or of the binding materials, the original friction coefficient could be reduced and sliding mechanism can occur, especially for the pointed vaults.

Furthermore the vaults are often schematized as arches side by side, which do not work together.

The results obtained by the limit state analysis with finite friction show that this schematisation, especially for complex vaults, do not provide information about the actual stress field. In fact, in the case of pavilion vaults, it is emerged the importance of the interaction between the arches for the evaluation of the crack pattern and the horizontal thrust.

Therefore, the present paper provide a new analysis tool for a computer procedure able to value both the rotational and sliding mechanisms, the three-dimensional effects in the vaults, very important especially for complex vaults and the vaults' safety factor, given by the minimum thickness over the actual thickness ratio.

ACKNOWLEDGEMENTS

The authors wish to thank Prof. Ezio Giuriani from the University of Brescia for suggesting the topic and providing critical insight during the development of this study.

REFERENCES

Amadei B. et al. 1995. Modelling the stability of masonry structures with the discontinuous deformation analysis (DDA) method. In *3dt International Symposyum on Computer Methods in Structural Masonry*, Lisbon.

Baggio C. & Trovalusci P. 1998. Limit analysis for no-tension and frictional three-dimensional discrete systems. *Mechanics of Structures and Machines* 26(3): 287–304.

Block P. et al. 2006. Real-time limit analysis of vaulted masonry buildings. *Computer and structure* 84(29–30): 1841–1852.

Boothby T. E. & Brown C. B. 1993. General lower and upper bound theorem of static stability, *Engineering Structures* 15(3): 189–196.

Boothby T. E. 1994. Stability of Masonry Piers and Arches Including Sliding. *Journal of Engineering Mechanics* 120(2): 304–319.

Boothby T. E. 1994. Limit states analysis of masonry arches. In *Proceedings of the Structures Congress '94, Atlanta, 24–28 April 1994*. ASCE.

Breymann G. A. 2003. *Archi, volte, cupole (1885)*. Roma: Dedalo.

Casapulla C. & D'Ayala D. 2001. Lower bound approach to the limit analysis of 3D vaulted block masonry structures. In *Computer Methods in Structural Masonry (STRUMAS V); Proc. 5th intern. symp., Roma, 18–20 April 2001*.

Cundall A. 1971. Formulation of three-dimensional distinct element model-part I: a scheme to detect and represent contacts in a system composed of masonry polyhedral blocks. *Int. J. Rock Mech. Min Sci. Geomech.* 25(3): 107–116.

Curioni G. 1870. *L'arte di Fabbricare. Costruzioni civili, stradali, idrauliche*. Torino: Negro.

D'Ayala D. 1994. In tema di comportamento strutturale delle cupole in muratura. *Ph.D. Thesis*, Dept. of "Ing. Strutt. e Geot.", Univ. "La Sapienza", Roma.

D'Ayala D. & Casapulla C. 2001 Limit state analysis of hemispherical domes with finite friction. In Lourenço P.B., Roca P. (Eds.). *Structural Analysis of Historical Constructions, Proc. intern. seminar, Guimaraes 7–9 November*. Guimaraes: Balkema.

Drucker D. C. 1954. Coulomb friction, plasticity and limit loads. *Journal of Applied Mechanics* 21(1): 71–74.

Ferris M. C. 2001. Limit analysis of frictional block assemblies as a mathematical program with complementarity constraints. *International Journal of Mechanical Sciences* 43(1): 209–224.

Gilbert M. & Melbourne C. 1994. Rigid-block analysis of masonry structures. *The structural engineering* 72(18): 356–361.

Gilbert M. et al. 2006. Limit analysis of masonry block structures with non-associative frictional joints using linear programming. *Computers and Structures* 84 (13–14): 873–887.

Giuriani E. et al. 2001, Structural rehabilitation of masonry vaults. In UNESCO-ICOMOS millennium congress; *Proc. intern. symp., Paris, 10–12 Septembre 2001*.

Giuriani E. et al. 2002. Studio del comportamento strutturale delle volte a padiglione in muratura. *Technical Report of University of Brescia* 17: 1–327.

Guarini G. 1968. *Architettura civile (1737)*. Milano: Il polifilo.

Harvey W. J. 1988. Application of the mechanism analysis to masonry arches. *The structural Engineer* 66(5), 77–84.

Heyman J. 1977. *Equilibrium of shell structures*, Oxford: Clarendon Press.

Heyman J. 1996. *Arches, Vaults and Buttresses*, Norfolk: Variorum.

Huerta S. 2001. Mechanics of masonry vaults: The equilibrium approach. In Lourenço P.B., Roca P. (Eds.), *Structural Analysis of Historical Constructions, Proc. intern. seminar, Guimaraes 7–9 November*. Guimaraes: Balkema.

Levi C. 1932. *Trattato teorico-pratico di costruzioni civili, rurali, stradali ed idrauliche*. Milano: Hoepli.

Livesley R. K. 1978. Limit Analysis of structures formed from rigid blocks. *International Journal for Numerical Methods in Engineering* 12(11): 1853–1871.

Livesley R. K. 1992. A computational model for the limit analysis of threedimensional masonry structures. *Meccanica* 27(3): 161–172.

Lourenço P. B. 1996. Computational strategies for masonry structures. Thesis Delft University of Technology. Delft University Press.

Lourenço P. B. 2001. Analysis of historical constructions: From thrust-lines to advanced simulations Historical Constructions. In Lourenço P.B., Roca P. (Eds.), *Structural Analysis of Historical Constructions, Proc. intern. seminar, Guimaraes 7–9 November*. Guimaraes: Balkema.

Lourenco P. B. 2006. Recommendations for restoration of ancient buildings and the survival of a masonry chimney. *Construction and Building Materials* 20(4): 239–251.

Nart M. 2003. Limit analysis of masonry domes. *Masonry international* 16(1): 12–20.

O'Dowyer D. 1999. Funicular analysis of masonry vaults. *Computer and Structures* 73(1–5): 187–197.

Oppenheim, I. J et al. 1989. Limit state analysis of masonry domes. *Journal of Structural Engineering* 115(4): 868–882.

Palladio A. 1980. *I quattro libri dell'architettura (1570)*. Milano: Il polifilo.

Scamozzi V. 1964. *L'idea dell'architettura universale (1615)*, Ridgewood: Gregg.

Smars P. 2000. Etudes sur la stabilité des arcs et voûtes, Ph.D. thesis, Department of Civil Engineering, Katholieke universiteit Leuven.

Tomasoni E. 2008. Le volte in muratura negli edifici storici: tecniche costruttive e comportamento strutturale. *Ph.D. Thesis*, DICATA, Università degli Studi di Brescia.